

RSC Advances



This article can be cited before page numbers have been issued, to do this please use: B. Gopal, P. Venkatesan, S. WU and V. Sivan, *RSC Adv.*, 2016, DOI: 10.1039/C5RA27517B.



This is an *Accepted Manuscript*, which has been through the Royal Society of Chemistry peer review process and has been accepted for publication.

Accepted Manuscripts are published online shortly after acceptance, before technical editing, formatting and proof reading. Using this free service, authors can make their results available to the community, in citable form, before we publish the edited article. This *Accepted Manuscript* will be replaced by the edited, formatted and paginated article as soon as this is available.

You can find more information about *Accepted Manuscripts* in the [Information for Authors](#).

Please note that technical editing may introduce minor changes to the text and/or graphics, which may alter content. The journal's standard [Terms & Conditions](#) and the [Ethical guidelines](#) still apply. In no event shall the Royal Society of Chemistry be held responsible for any errors or omissions in this *Accepted Manuscript* or any consequences arising from the use of any information it contains.



Novel Ratiometric Turn-on Fluorescent Probe for Selective Sensing of Cyanide ions, Effect of substitution and Bio-imaging Studies

Gopal Balamurugan^a, Parthiban Venkatesan^b, Shu Pao Wu^b, Sivan Velmathi^{a,*}

Received 00th January 20xx,
Accepted 00th January 20xx

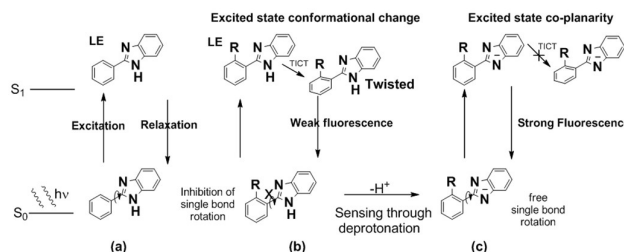
DOI: 10.1039/x0xx00000x

www.rsc.org/

Novel fluorogenic receptors **S1-S4** (imidazo anthraquinone derivatives) were synthesized from *o*-substituted benzaldehyde and 1,2-diaminoanthraquinone and characterised well with various spectroanalytical techniques. In case of **S1**, the selectivity towards cyanide ions with turn on fluorescence output among other anions due to the inhibition of twisted intramolecular charge transfer (TICT) mechanism. Effect of substitution was successfully compared with sensing studies of **S2-S4**. **S1** showed good binding constant with 1:1 stoichiometric ratio and micromolar detection limit. The sensing behaviour was further supported by ¹H NMR Titration, TD-DFT calculations and lifetime measurement studies. **S1** was applied for the bio-imaging of the cell line RAW264.7 and successfully sensed the cyanide ions in the physiological conditions.

Introduction

Cyanide ion is highly toxic and severe health hazard anion that could be lethal dose for human beings even as low as 1.5 mg/kg of body weight. Consequently, the utmost tolerant level of cyanide in drinking water was set at 1.9 μM by the World Health Organization (WHO). The inhibition of *cytochrome-c-oxidase* in the mitochondria of the eukaryotic cells has been occurred by cyanide ions due to the rapid coordination with the iron center led to the inhibition of oxygen intake by the cells of an organism¹. Because of the extensive usage of cyanide worldwide in industries such as Gold mining (cyanide leaching process), electroplating, refineries (fluid catalytic cracking and coking), printed circuit board manufacturing, steel and chemical industries, the environmental pollution could not be outmanoeuvred entirely¹⁻⁴. By considering the above facts, a center of attention has been created for the articulate design and synthesis of efficient probes to selectively detect CN⁻ at the environmental and biological medium. There are surplus of articles published for bio-imaging of cyanide anion (CN⁻) in the cells based on the strategies such as the formation of cyanide complexes^{5, 6}, nucleophilic addition of CN⁻ to activated double bond or a boron center and relay recognition⁷⁻¹⁸. Recently, anthraquinone based imidazole receptors have been reported for the detection of anions and metal ions.¹⁹⁻²⁶ In most of the cases, imidazole based receptors performed as colorimetric sensors and very few of them showed fluorescence turn off behaviour. Fluorescent off-on imidazo anthraquinone probes for cyanide may not be prominent in the picture. From the clear literature review over the structural aspects like chromophore, fluorophore, electron withdrawing and donating substituents in the imidazole based receptors, we could achieve the fluorescent enhancement for the anions based on Twisted Intra



Scheme 1: Design strategy using TICT mechanism.

Molecular Charge Transfer (TICT) mechanism²⁷⁻³⁰. A clear picture of the TICT process in case of 2'-substituted imidazole in the ground state and excited state was shown in scheme 1. (a) Free rotation could be possible in case of no substitution. The presence of substitution in 2' position inhibit the rotation as well in the excited state (S₁), (b) intramolecular charge transfer took place as TICT process followed by the relaxation to the ground state (S₀) (c) But the deprotonation of the imidazole -NH may liberate the steric hindrance followed by the inhibition of TICT process resulted in the enhanced fluorescence. Based on this strategy, we designed the receptor **S1**, synthesized in good yield and characterized well with various spectroscopic techniques, sensing studies towards the highly toxic anions and biological important anions. Further supporting information to prove the sensing behaviour and fluorescence enhancement were obtained using UV-vis, photoluminescence and ¹H NMR titration, fluorescence life measurement and DFT calculation. Effect of substitution using electron donating group was also performed by synthesizing **S2-S4** to precise the sensing behaviour of **S1**. Binding constants, detection limit and quantum yield were thoroughly determined for the receptors. To reach the ultimate destination of chemosensors, **S1** was applied lucratively for real time selective detection of cyanide ions in domestic waste water. Ultimately, **S1** was successfully applied for bio-imaging of RAW264.7 cell lines.

^a Organic and polymer synthesis Laboratory, Department of Chemistry, National Institute of Technology, Tiruchirappalli-620015, India.

^b Department of Applied Chemistry, National Chiao Tung University, Hsinchu, Taiwan

ARTICLE

RSC Advances

Scheme 2: Syntheses of *o*-substituted imidazo anthraquinone derivatives S1-S4.

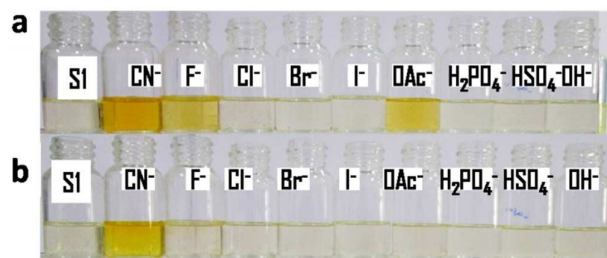
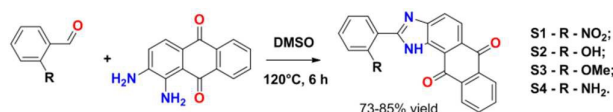


Fig. 1 (a) 200 μL of anions (1.5×10^{-3} M in ACN) was added in 3 mL of S1 (5×10^{-5} M in ACN) (b) 200 μL of anions (1.5×10^{-3} M in H_2O) was added in 3 mL of S1 taken in 97:3 ACN: water.

Reagents and Instruments

1,2-Diaminoanthraquinone (DAAQ), 2-nitrobenzaldehyde were purchased from Sigma Aldrich and utilized without further purification. Tetrabutylammonium (TBA) salts of anions such as CN^- , F^- , Cl^- , Br^- , I^- , OAc^- , H_2PO_4^- , HSO_4^- , OH^- and analytical grade solvents were purchased commercially and used as such. NMR spectra were obtained using a Bruker 500 MHz spectrometer using Tetramethylsilane (TMS) as an internal standard. Thermo Fisher FT IR Spectrometer was used to record IR spectra in pellet mode. UV-vis spectroanalysis were done on Shimadzu UV-2600 UV-vis spectrophotometer in quartz cell with 1 cm path length. Photoluminescence spectra were recorded using Shimadzu RF-5301PC spectrophotometer. 1.5×10^{-3} M aq. solutions of the anions with 5×10^{-5} M solutions of S1 in ACN medium had been utilized for the studies. UV titrations were carried out by the incremental addition of 0.1 eq. (10 μL) - 2 eq. (200 μL) of guest solutions to 3 mL of receptor solution in the UV cuvette. ^1H NMR titration was carried out using 0.1 M solution of TBACN in DMSO-d_6 and 0.01 M solution of S1 in DMSO-d_6 in Bruker Avance III 500 MHz NMR Spectrometer. Life time measurement studies were done at Horiba Delta time instrument coupled with TCSPC. Confocal fluorescence imaging of cells was performed with a Leica TCS SP5 X AOBs Confocal Fluorescence Microscope (Germany), and a 63x oil-immersion objective lens was used. The cells were excited with a white light laser at 456 nm, and emission was collected at $540 \pm 580\text{nm}$. DFT calculation was performed using Gaussian 09 software package and the optimized structures and MOs were processed from GaussView 5.0 package.

Synthesis of *o*-substituted anthra[1,2-d]imidazole-6,11-dione (S1-S4):

o-substituted benzaldehyde (0.5 mmol) and 1,2-diaminoanthraquinone (0.5 mmol) were taken in DMSO (1 mL) and heated to 120°C for 6 h. (Scheme 2) The completion of the reaction was monitored by thin layer chromatography (TLC) using hexane: ethylacetate (6:4) as an eluent. After cooling the reaction mixture

to room temperature, cold ethanol (5 mL) was added and stirred for few minutes. The solid obtained was filtered, washed with ethanol (5 mL x 3), dried. The crude product obtained was again triturated with hot ethanol (5 mL) to yield pure receptor.

2-(2-nitrophenyl)-1H-anthra[1,2-d]imidazole-6,11-dione (S1)

Yield: 73%. M.p. $248-250^\circ\text{C}$. ^1H NMR 500 MHz, DMSO-d_6 : δ 13.85 (s, 1H), 8.28-8.29 (m, 4H), 8.22 (dd, $J = 8.50, 32.00$ Hz, 2H), 8.01-8.02 (m, 2H), 8.02 (dd, $J = 8.00, 23.75$ Hz, 2H), 7.92 (t, $J = 7.50$ Hz, 1H). ^{13}C NMR (75 MHz, DMSO-d_6) 120.17, 124.91, 125.46, 125.84, 126.1, 127.27, 128.87, 132.07, 133.30, 133.43, 133.53, 133.74, 134.74, 134.93, 149.01, 155.46, 182.90, 183.50. FTIR ($\nu\text{-cm}^{-1}$) 3427 (N-H str.), 1666 (C=O str.), 1537 (Nitro asymmetric), 1476 (C=N str.), 1365 (Nitro asymmetric), 715 (N-H bending) HRMS: Calcd. for $\text{C}_{21}\text{H}_{12}\text{N}_2\text{O}_4$: m/z 369.075. Found: m/z 370.083(M+1).

2-(2-hydroxyphenyl)-1H-anthra[1,2-d]imidazole-6,11-dione (S2)

Yield: 85%. M.p. $265-267^\circ\text{C}$. ^1H NMR 500 MHz, DMSO-d_6 : δ 12.65 (s, 1H, -OH), 11.96 (s, 1H, -NH), 8.461-8.269 (m, 2H), 8.177-8.088 (m, 2H), 8.044-7.944 (m, 2H), 7.882-7.797 (m, 1H), 7.38 (t, $J = 7.30$ Hz, 1H), 7.04 (d, $J = 8.10$ Hz, 1H), 6.98 (t, $J = 7.35$ Hz, 1H). ^{13}C NMR (75 MHz, DMSO-d_6) 117.56, 118.35, 120.29, 121.67, 124.82, 126.70, 127.26, 128.23, 129.55, 133.31, 134.65, 134.96, 156.63, 157.42, 182.58. FTIR ($\nu\text{-cm}^{-1}$) 3548 (O-H str.), 3442 (N-H str.), 1660 (C=O str.), 1476 (C=N str.), 715 (N-H bending) HRMS: Calcd. for $\text{C}_{21}\text{H}_{12}\text{N}_2\text{O}_4$: m/z 340.332. Found: m/z 341.071(M+1).

2-(2-methoxyphenyl)-1H-anthra[1,2-d]imidazole-6,11-dione (S3)

Yield: 78%. M.p. $233-236^\circ\text{C}$. ^1H NMR 500 MHz, DMSO-d_6 : δ 12.35 (s, 1H), 8.50 (d, $J = 6.50$ Hz, 1H), 8.22-8.42 (m, 2H), 8.06 (dd, $J = 8.00, 32.25$ Hz, 2H), 7.74-7.82 (m, 2H), 7.55 (t, 1H), 7.33 (d, $J = 7.50$ Hz, 1H), 7.16 (d, $J = 7.00$ Hz, 1H), 4.28 (s, 3H). ^{13}C NMR (75 MHz, DMSO-d_6) 57.11, 113.24, 121.54, 121.99, 125.30, 126.80, 127.42, 130.32, 132.52, 133.54, 134.75, 135.16, 155.46, 158.00, 184.56. FTIR ($\nu\text{-cm}^{-1}$) 3485 (N-H str.), 1668 (C=O str.), 1472 (C=N str.), 1054 (-OMe), 714 (N-H bending) HRMS: Calcd. for $\text{C}_{21}\text{H}_{12}\text{N}_2\text{O}_4$: m/z 354.358. Found: m/z 355.140 (M+1).

2-(2-aminophenyl)-1H-anthra[1,2-d]imidazole-6,11-dione (S4)

Yield: 81%. M.p. $248-250^\circ\text{C}$. ^1H NMR 300 MHz, DMSO-d_6 : δ 12.43 (s, 1H), 8.13 (s, 2H), 7.99-0.00 (m, 2H), 7.89-7.91 (m, 2H), 7.16-7.24 (m, 2H), 7.21 (d, $J = 6.60$ Hz, 1H), 6.87 (d, $J = 6.00$ Hz, 1H), 6.68 (d, $J = 6.60$ Hz, 1H). ^{13}C NMR (75 MHz, DMSO-d_6) 116.66, 118.11, 119.05, 121.38, 124.28, 126.68, 127.11, 128.02, 129.02, 132.18, 133.34, 134.74, 134.70, 149.52, 182.52, 183.49. FTIR ($\nu\text{-cm}^{-1}$) 3432 (N-H str.), 1661 (C=O str.), 1469 (C=N str.), 1102 (C-N str.), 715 (N-H bending) HRMS: Calcd. for $\text{C}_{21}\text{H}_{12}\text{N}_2\text{O}_4$: m/z 339.105. Found: m/z 340.086(M+1).

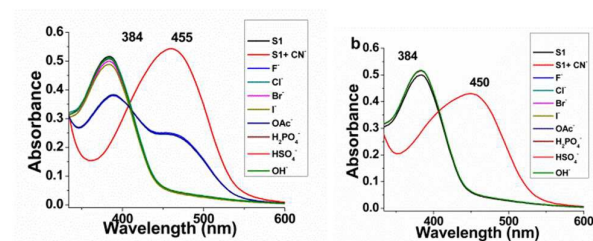


Fig. 2 (a) UV-vis spectral studies of **S1** (5×10^{-5} M in ACN) with $200 \mu\text{L}$ of anions (1.5×10^{-3} M in ACN) (b) UV-vis spectral studies of **S1** (5×10^{-5} M in 97:3 ACN: water) with $200 \mu\text{L}$ of anions (1.5×10^{-3} M in H_2O)

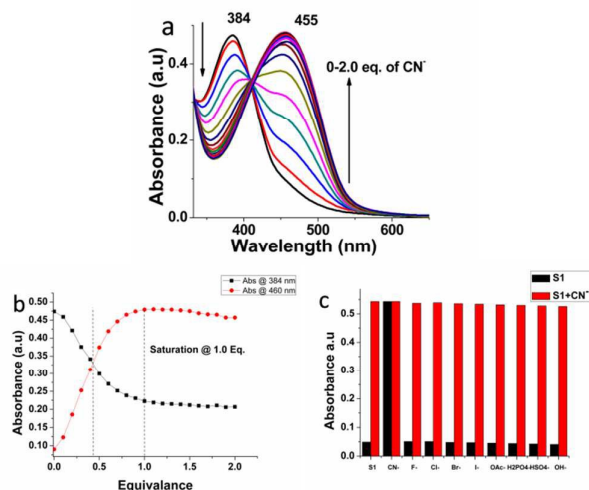


Fig. 3 (a) Incremental addition of CN^- to **S1** (b) Support for the ratiometric detection of CN^- by **S1** with 1:1 stoichiometric ratio (c) Interference of other anions in the sensing behaviour of **S1** with cyanide ions.

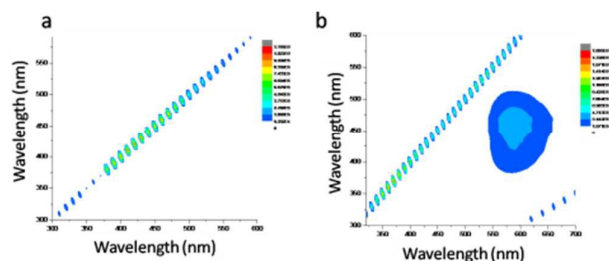


Fig. 4 (a) 2D contour image of Photoluminescence **S1** (b) S1^-

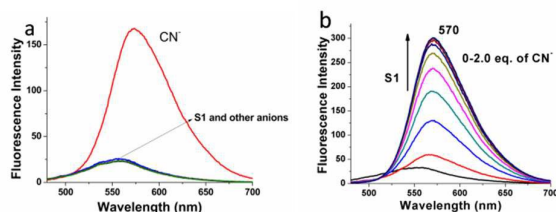


Fig. 5 (a) Photoluminescence studies of **S1** (5×10^{-5} M in 97:3 ACN: water) with $200 \mu\text{L}$ of Anions (1.5×10^{-3} M in H_2O) (b) Photoluminescence studies of the incremental addition of CN^- to **S1**.

Results and Discussion

Naked eye sensing

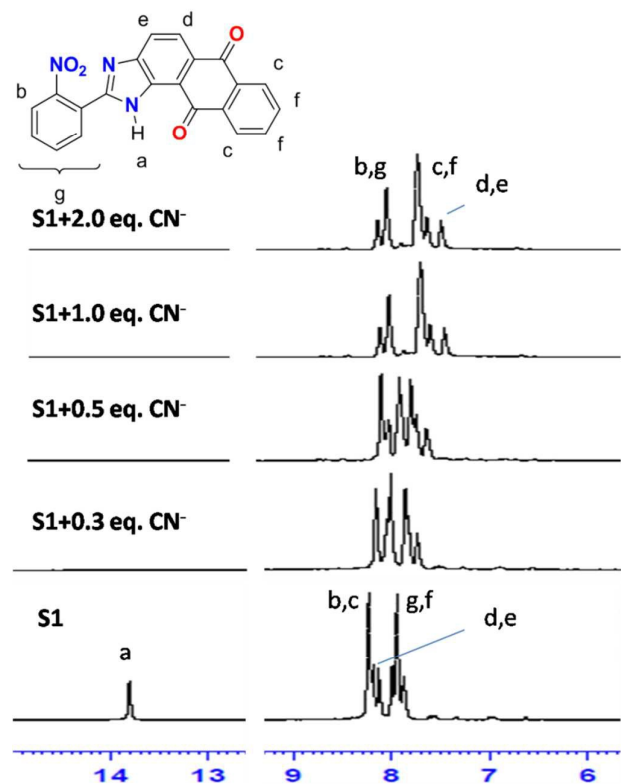
Initially, $200 \mu\text{L}$ of anions, CN^- , F^- , Cl^- , Br^- , I^- , OAc^- , H_2PO_4^- , HSO_4^- & OH^- (1.5×10^{-3} M in ACN) were added to 3 mL of **S1-S4** (5×10^{-5} M in ACN) to examine the sensitivity visually. **S1** (Fig. 1a), **S2** and **S4** were shown strong color change for CN^- ions whereas F^- and OAc^- ions showed slight colour change. But **S3** did not show any color change, this may be furnished as the electron donating $-\text{OMe}$ in **S3** decrease the acidity of the imidazole $-\text{NH}$. (Supporting information fig. A1) By taking into account the compatibility of the receptor with water to analyze the environmental measures, anions were taken in H_2O for further analysis. Interestingly, **S1** showed the intense yellow color change selectively for cyanide among anions. To increase the ecological factor, the percentage of water in ACN for **S1** had been altered and it showed intense yellow color change only for cyanide ions in 3% Aq. ACN medium (Fig. 1b). No sensing was observed above 3% aq. ACN solution of **S1**. In the same way, **S2** and **S4** were displayed the same result alike **S1**. (Supporting Information fig. A1)

UV-vis spectral studies

By analyzing the sensing behaviour using UV-vis spectroscopy, under 100% ACN medium, **S1** showed an absorbance maxima at 384 nm and the addition of cyanide ion into **S1** suppress the corresponding band and formed a new band at 460 nm whereas fluoride and acetate ions interact with **S1** weakly compared to cyanide. (fig. 2a) This proves the higher nucleophilicity of cyanide played a vital role in the sensing behaviour. While using aq. solution of anions to **S1** in ACN, due to the effect of solvation by water molecules, cyanide ions only showed the bathochromic shift to 450 nm. (fig. 2b) As we saw in the naked eye experiment, beyond 10% of water content in ACN, no shift was observed. The incremental addition of cyanide ions ($20\text{--}200 \mu\text{L}$) to **S1** clearly exposes the gradual decrease in the band at 384 nm and increase in the band at 455 nm. (fig. 3a) The ratiometric behaviour of **S1** towards cyanide ions could be helpful to quantitatively analyze the same in the real sample by using Beer-Lambert's law. (fig. 3b) Interference of other anions towards cyanide sensing of **S1** was demonstrated successfully that shows there is no effective interference in the absorbance maxima of **R1-CN** complex. (fig. 3c) In case of **S2** and **S4** band at 410 nm and 448 nm were red-shifted to 480 nm and 500 nm respectively. (Supporting Information fig. A2, A3). Using Benesi-Hildebrand plot, from the incremental addition of CN^- ions to **S1**, **S2** and **S4**, **S1** displayed a very good association constant (1.5×10^4) whereas **S2** and **S4** showed slightly lesser binding constants. By using Job's plot, the stoichiometric ratio of the guest-host complexes were calculated and listed in table 1. Except **S2**, others possess 1:1 stoichiometry. Both the binding sites in **S2** ($-\text{OH}$ and imidazole $-\text{NH}$) were deprotonated to give 1:2 host:guest stoichiometric ratio. In addition, detection limit and limit of quantification were also calculated for the receptors. All the experiments were reiterated to assure the repeatability and confirmed with the low error percentage.

Table 1: Binding constant, detection limit and stoichiometric ratio of the host-guest complexes formed.

Species	Binding Constant	Detection Limit LOD	Limit of Quantification LOQ	Stoichiometric Ratio
S1-CN ⁻	15466	3.960 x 10 ⁻⁶ M	1.31 x 10 ⁻⁵ M	1:1
S2-CN ⁻	13862	2.96 x 10 ⁻⁶ M	9.87x10 ⁻⁶ M	1:2
S4-CN ⁻	7103	7.25 x 10 ⁻⁷ M	2.41 x 10 ⁻⁶ M	1:1

**Fig. 6** ¹H NMR titration of **S1** (0.01 M in DMSO-d₆) with cyanide ion (0–2.0 eq. of 0.1 M in DMSO-d₆)

Fluorescence spectral studies

3D fluorescence spectral study was carried out to prop up the effective fluorogenic sensing of cyanide by **S1**. The fluorescence property of the receptor **S1** was investigated by using 3D scan recording emission spectra from 300 to 600 nm while the excitation was subsequently tuned from 300 to 600 nm. The contour image of the spectra of the receptor showed very weak fluorescence whereas after the addition of cyanide to the receptor, there was a new band formed around λ_{em} 570 - 625 nm range in the excitation wavelength of (λ_{ex}) 425 - 475 nm (Fig 4a, b). The photoluminescence spectral studies were carried out with the excitation at 455 nm and the slit width of 5 nm. **S1** showed very weak fluorescent and an emission peak at 554 nm. Among various anions, only for the addition of cyanide ion, **S1** displayed 10-fold fluorescent enhancement with a bathochromic shift from 554 nm to 570 nm (Fig 5a, b). It could be inferred from the results that the coplanarity of the system was retained by the deprotonation of 1-H of imidazole moiety of **S1** followed by the fluorescence enhancement via the inhibition of twisted intramolecular charge transfer (TICT) mechanism. **S2** was excited with 500 nm and emission was observed at 558 nm by adding cyanide ions into **S2**, fluorescence quenching took place whereas in case of **S4**, comparatively

fluorescent enhancement was observed. (Supporting Information fig. A3) It can be inferred from the above the observation that the introducing bulkier electron withdrawing group in the 2' position of phenyl ring will induce the fluorescent enhancement through TICT process.

Quantum yield

Quantum Yield of **S1** and deprotonated form of **S1**(**S1**) have been calculated by using the following method with Rhodamine-B as a reference(R).

$$\frac{\Phi_S}{\Phi_R} = \frac{I_S}{I_R} \times \frac{(1 - 10^{-A_R})}{(1 - 10^{-A_S})} \times \frac{n_S^2}{n_R^2} \quad (\text{Equation 1})$$

Φ_S – Quantum Yield of the sample; Φ_R – Quantum yield of the reference (Quantum yield of Rhodamine B is 0.68 in EtOH); I – Fluorescence intensities of the sample (S) and reference(R); A – Uv-vis absorbance of the sample (S) and reference(R); n – Refractive Index of the solvent used (For EtOH - 1.36 and for DMSO – 1.47); As quantum yield is temperature dependent, in both the cases temperature was maintained same. By applying the experimental value in the equation 1, quantum yields of **S1** and **S1**+CN⁻ were found to be 0.0033 and 0.033 in DMSO. 10-fold enhancement clearly tells the efficient usage of the receptor **S1** as a selective fluorescent probe.

¹H NMR Titration

The recognition of cyanide by **S1** can further be supported by ¹H NMR titration (fig 6). 0.01 M solution of **S1** and 0.3–2.0 eq of TBACN (0.1 M in DMSO-d₆) were used for the ¹H NMR titrations. Highly acidic in nature and the ability to interact through hydrogen bonding of the –OH and imidazole NH with cyanide drives the proton to appear at down field. Due to the addition of cyanide ion with the receptor, the peak at 13.85 ppm (a) corresponding for imidazole –NH, was disappeared. On increasing the concentration of cyanide, the shifting of the peaks at 7.8–8.0 ppm (c-f protons) were shifted to 7.4–7.8 ppm belonged to the anthraquinone protons and the protons (b and g) in the nitrophenyl ring were remained same. As the deprotonation occurred during the addition of cyanide ions, the electron density around anthraquinone moiety might be increased and resulted in the local diamagnetic shielding of the corresponding protons. But the electron density around nitrophenyl ring may not be altered much by the deprotonation process therefore no change was observed in the corresponding protons of the same.

Life Time Measurement

Further, time dependent photoluminescence decay process had been carried out for the life time measurement of **S1** and **S1**-CN ion pair complex. A pinch of milk powder in water had been used to

prompt the instrument. The proposed mechanism was also well propped up by the fluorescence lifetime data. In the fluorescence

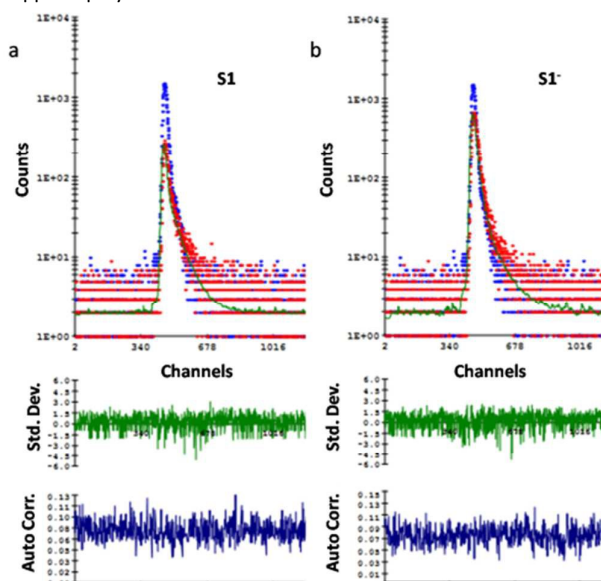


Fig.7 Lifetime measurement studies of **S1** (a) and **S1⁻** (b)

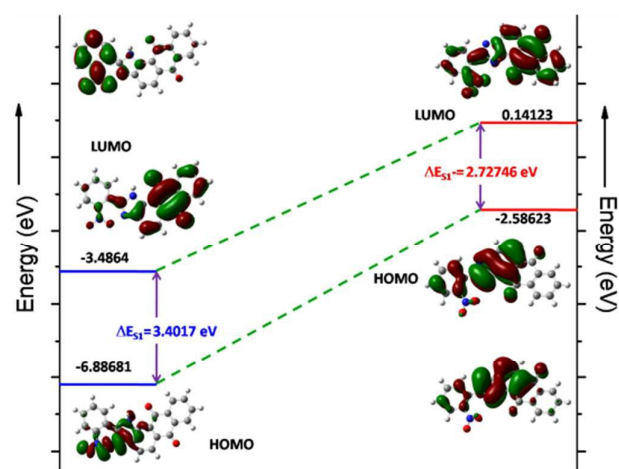


Fig.8 DFT Theoretical studies using Gaussian 09 software with B3LYP 6-31G basis set of **S1** and **S1⁻**.

Table 2: The comparison of experimental and theoretical λ_{max} of **S1** and **S1⁻** using TD-DFT Studies.

Species	Calculated λ_{max} (nm)	Experimental λ_{max} (nm)
S1 and S1⁻	382.12/455.33	384/455
S2 and S2⁻	380.76/495.22	410/480
S4 and S4⁻	380.97/521.00	443/500

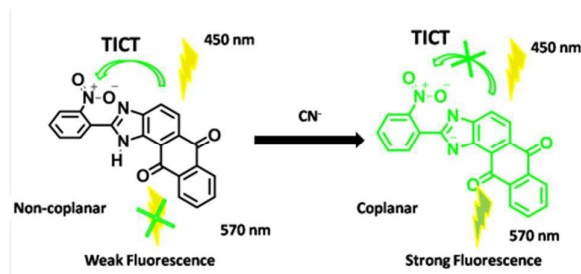


Fig. 9: The proposed mechanism for the sensing behaviour of **S1**

lifetime decay experiment ($\lambda_{\text{em}} = 554 \text{ nm}$), the average luminescence lifetime of **S1** was found to be 3.5 ns at which 455 nm nanoLED source was used. After the addition of 10 μM of CN^- ions to the solution of **S1**, the average luminescence lifetime ($\lambda_{\text{em}} = 570 \text{ nm}$) of **S1-CN** system increased to 4.7 ns. In both the cases, the fluorescence decay curve was fitted to double-exponential decay theoretical calculation. From the obtained results, there is a delay (1.5 ns) in the decay process when cyanide ion interacts with the receptor; hence it is proved that there is a platform for the enhanced fluorescence in the case **S1-CN⁻** interaction. (Fig. 7a, b)

DFT theoretical calculations

DFT theoretical calculations were demonstrated for **S1** and **S1⁻** for supporting the deprotonation occurred during the addition of cyanide ion. The structural optimization and the computational calculations were carried out using Gaussian09 quantum chemistry package and the results were viewed with GaussView5 GUI.³¹ Geometry optimizations were conducted by DFT using Becke's three parameter exchange functional (B3)³² and includes a mixture of HF with DFT exchange terms associated with the gradient corrected correlation functional of Lee, Yang, and Parr (LYP)^{29,33} and the 6-31G basis set. Highest occupied molecular orbital (HOMO) and lowest unoccupied molecular orbital (LUMO) for **S1** and its deprotonated form (**S1⁻**) have been generated from optimized structures of the same (fig. 8). From the calculated results, the energy gap between HOMO and LUMO of **S1** had decreased after deprotonation of $-\text{NH}$ of imidazole by cyanide ions. The calculated absorbance maxima of **S1** and **S1⁻** from the energy gap (ΔE_{S1} and ΔE_{S1^-}) were 364 nm and 454 nm respectively and well coincided with the experimental values. From the TD-DFT studies of the receptors **S1**, **S2** and **S4** and their corresponding deprotonated form **S1⁻**, **S2⁻** and **S4⁻** were carried out with TD-SCF CAM-B3LYP with the basis set 6-31G (keyword- td cam-b3lyp/6-31g geom=connectivity). From the results, it could be concluded that the experimental λ_{max} of the receptors and their respective deprotonated forms were well agreed with those of calculated λ_{max} which further supports the sensing behaviour of the receptor. (Table 2)

Mechanism

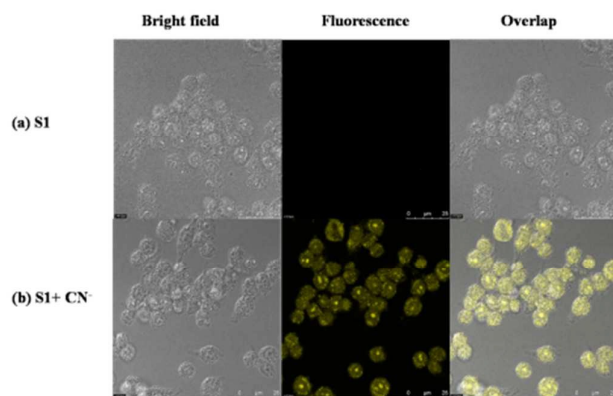
From ^1H NMR spectral titration, DFT Calculation and life time measurement studies, **S1** was deprotonated at $-\text{NH}$ imidazole by cyanide ions and the electron density over benzimidazo anthraquinone (chromophore) moiety was increased that driven the color change. The phenomenon was simply illuminated by the following statements; the bulkier nitro group in the *o*-position and 1-H of imidazole tend to disturb the co-planarity of the molecule whereas the co-planarity may be achieved in the excited state on deprotonation of the same followed by the fluorescence

ARTICLE

RSC Advances

Table 3: Real sample analysis of **S1** using waste water sample.

Sample (ppm)	Average Recovery (ppm)	% Recovery
0	0	Nil
5	4.3	86%
10	9.2	92%
15	14.4	96%

**Fig. 10** Fluorescence images of macrophage (RAW 264.7) cells treated with **S1** (a) and CN^- (b) ions. (Left) Bright field image; (Middle) fluorescence image; and (Right) merged image. (Ex 456nm, Em.540-580nm.)

enhancement; In other words, the higher electron withdrawing nature of nitro group makes the phenyl ring as an acceptor and there will be a Twisted Intramolecular Charge transfer (TICT) from electron rich imidazoanthraquinone moiety to nitrophenyl ring in **S1** whereas the deprotonation inhibits the TICT followed by the fluorescent enhancement. (Fig. 9)

Real Sample Analysis

Role of a chemosensor could be accomplished only when it might be useful in practical applications. Sensing cyanide ions in waste water collected in our premises was demonstrated with **S1**. The samples were collected every one hour and mixed with together. The resulting turbid sample as a whole was filtered to remove the suspended particle led to a light grey solution (pH 8.0). On testing the filtered sample with **S1**, no color change was observed. 5, 10 and 15 ppm cyanide solutions prepared from the filtered water samples were added with **S1**. The color change as well as bathochromic shift in the UV-vis spectra were observed. From the absorbance at 455 nm of the three solutions, using Beer-Lambert's Law, the corresponding concentrations were calculated for all the solutions. Overall 90% recovery was observed it could be concluded that **S1** acts as a highly sensitive and selective chemoreceptor for CN^- ion (Table 3).

Fluorescence imaging of Living Cells

The cell line RAW264.7 was provided by the Food Industry Research and Development Institute (Taiwan). RAW264.7 cells were cultured in Dulbecco's modified Eagle's medium (DMEM) supplemented with

10% fetal bovine serum (FBS) at 37 °C under an atmosphere of 5% CO_2 . Cells were plated on 18 mm glass coverslips and allowed to adhere for 24 h. Experiments to assess CN^- ions uptake were performed in PBS with 10 μM $(\text{CH}_3\text{CH}_2\text{CH}_2\text{CH}_2)_4\text{N}(\text{CN})$. Treated the cells with 2 μL of 10 mM CN^- ions (final concentration: 10 μM) dissolved in sterilized PBS (pH 7.4) and incubated for 30 min at 37°C. The treated cells was washed PBS (3 \times 2 mL) to remove remaining $(\text{CH}_3\text{CH}_2\text{CH}_2\text{CH}_2)_4\text{N}(\text{CN})$ ions. Culture media (2 mL) was added to the cell culture, which was treated with a 10 mM solution of **S1** (2 μL ; final concentration: 10 μM) dissolved in DMSO. The samples were incubated at 37°C for 30 min. The culture media was removed, and the treated cells were washed with PBS (3 \times 2 mL) before observation. (Fig. 10) From the images, it could be inferred that **S1** has very good permeability through the cell membrane and has very weak fluorescence whereas after the addition of cyanide ions, **S1** sensed the guest selectively with enhanced yellowish green fluorescent.

Conclusion

Novel TICT based fluorescent turn on probe **S1** was synthesized from 2-nitrobenzaldehyde and 1,2-diaminoanthraquinone and characterized well with various spectroanalytical techniques. Cyanide ions were selectively sensed by **S1** through the deprotonation of 1-H imidazole followed by the inhibition of TICT occurred led to 10-fold fluorescent enhancement. Effect of substitution was discussed using **S2-S4**. In case of **S2**, fluorescence quenching was observed due to the deprotonation of both the sites (-OH and imidazole -NH). But **S4** showed sufficient bulkiness to give slight fluorescent enhancement. **S1** showed relatively very good association constant with 1:1 stoichiometric ratio and micromolar detection limit. ^1H NMR titration clearly supported the deprotonation of 1-H imidazole and the sensing behaviour was further supported by DFT as well as TD-DFT studies. Moreover, lifetime measurement showed that there is a delay (1.5 ns) in double exponential decay of **S1** and **S1** $^-$ which was essential information for the fluorescence enhancement behaviour. **S1** was successfully applied for the real time analysis of waste water and the bio-imaging of the cell line RAW264.7 and sensed the cyanide ions with yellowish green fluorescence output under physiological conditions.

Acknowledgement

Author GB thanks UGC (University Grant Commission, India) for the financial support through Junior Research Fellowship scheme (F.2-8/2011(SA-1) dated 29/11/2013).

References

1. D. Shan, C. Mousty and S. Cosnier, *Anal. Chem.*, 2004, **76**, 178-183.
2. G. Miller and C. Pritsos, Cyanide: Soc., Ind. Econ. Aspects, Proc. Symp. Annu. Meet. TMS, 2001.
3. S. S. Chadwick, *Ullmann's Encyclopedia of Industrial Chemistry, Reference Services Review*, 1988, **16**, 31-34.
4. O. L. Hung and L. Nelson, *Tintinalli's Emergency Medicine: A Comprehensive Study Guide*, McGraw-Hill New York, 2004.
5. X. Lou, D. Ou, Q. Li and Z. Li, *Chem. Commun.*, 2012, **48**, 8462-8477.

6. M. Wenzel, J. R. Hiscock and P. A. Gale, *Chem. Soc. Rev.*, 2012, **41**, 480-520.
7. C. Männel-Croisé and F. Zelder, *Inorg. Chem.*, 2009, **48**, 1272-1274.
8. P. Anzenbacher, D. S. Tyson, K. Jursíková and F. N. Castellano, *J. Am. Chem. Soc.*, 2002, **124**, 6232-6233.
9. K.-S. Lee, H.-J. Kim, G.-H. Kim, I. Shin and J.-I. Hong, *Org. Lett.*, 2008, **10**, 49-51.
10. J. Zhao, S. Ji, Y. Chen, H. Guo and P. Yang, *Phys. Chem. Chem. Phys.*, 2012, **14**, 8803-8817.
11. S. K. Kwon, S. Kou, H. N. Kim, X. Chen, H. Hwang, S. W. Nam, S. H. Kim, K. M. K. Swamy, S. Park and J. Yoon, *Tetrahedron Lett.*, 2008, **49**, 4102-4105.
12. S.-W. Nam, X. Chen, J. Lim, S. H. Kim, S.-T. Kim, Y.-H. Cho, J. Yoon and S. Park, *PLoS ONE*, 2011, **6**, e21387.
13. M. K. Bera, C. Chakraborty, P. K. Singh, C. Sahu, K. Sen, S. Maji, A. K. Das and S. Malik, *J. Mater. Chem. B*, 2014, **2**, 4733-4739.
14. S. Madhu, S. K. Basu, S. Jadhav and M. Ravikanth, *Analyst*, 2013, **138**, 299-306.
15. C. H. Lee, H. J. Yoon, J. S. Shim and W. D. Jang, *Chem. Eur. J.*, 2012, **18**, 4513-4516.
16. D. Kim, S.-Y. Na and H.-J. Kim, *Sens. Actuators B: Chem.*, **226**, 227-231.
17. S.-Y. Na and H.-J. Kim, *Tetrahedron Lett.*, 2015, **56**, 493-495.
18. M. Yoo, S. Park and H.J. Kim, *Sens. Actuators B: Chem.*, 2015, **220**, 788-793.
19. L. Yang, X. Li, Y. Qu, W. Qu, X. Zhang, Y. Hang, H. Ågren and J. Hua, *Sensor. Actuat. B-Chem*, 2014, **203**, 833-847.
20. M. Sun, S. Wang, Q. Yang, X. Fei, Y. Li and Y. Li, *RSC Adv.*, 2014, **4**, 8295-8299.
21. R. M. Batista, S. P. Costa and M. M. M. Raposo, *Sensor. Actuat. B-Chem*, 2014, **191**, 791-799.
22. R. M. Batista, S. P. Costa and M. M. M. Raposo, *J. Photochem. Photobiol. A: Chem.*, 2013, **259**, 33-40.
23. N. Kumari, S. Jha and S. Bhattacharya, *J. Org. Chem.*, 2011, **76**, 8215-8222.
24. B. Wannalarse, T. Tuntulani and B. Tomapatanaget, *Tetrahedron*, 2008, **64**, 10619-10624.
25. S. Suganya, J. S. Park and S. Velmathi, *J. Fluoresc.*, 2016, **26**, 207-215.
26. G. Balamurugan and S. Velmathi, *Anal. Methods*, 2016, **8**, 1705-1710.
27. K. Rotkiewicz, H. Leismann and W. Rettig, *Journal of Photochemistry and Photobiology, A: Chemistry*, , 1989, **49**, 347 - 367.
28. A. Maliakal, G. Lem, N. J. Turro, R. Ravichandran, J. C. Suhadolnik, A. D. DeBellis, M. G. Wood and J. Lau, *J. Phys. Chem. A*, 2002, **106**, 7680-7689.
29. Q. Li, M. Peng, H. Li, C. Zhong, L. Zhang, X. Cheng, X. Peng, Q. Wang, J. Qin and Z. Li, *Org. Lett.*, 2012, **14**, 2094-2097.
30. V. Tharmaraj and K. Pitchumani, *Anal. Chim. Acta*, 2012, **751**, 171-175.
31. M. Frisch, G. Trucks, H. B. Schlegel, G. Scuseria, M. Robb, J. Cheeseman, G. Scalmani, V. Barone, B. Mennucci and G. Petersson, *Inc., Wallingford, CT*, 2009, **200**.
32. A. Zaitsevskii, E. Rykova, N. Mosyagin and A. Titov, *Open Phys.*, 2006, **4**, 448-460.
33. C. Lee, W. Yang and R. G. Parr, *Phys. Rev. B*, 1988, **37**, 785.

Novel Ratiometric Turn-on Fluorescent Probe for Selective Sensing of Cyanide ions, Effect of substitution and Bio-imaging Studies

Gopal Balamurugan^a, Parthiban Venkatesan^b, Shu Pao Wu^b, Sivan Velmathi^{a,*}

^aOrganic and polymer synthesis Laboratory, Department of Chemistry, National Institute of Technology, Tiruchirappalli-620015, India.

^bDepartment of Applied Chemistry, National Chiao Tung University, Hsinchu, Taiwan

*Corresponding Author velmathis@nitt.edu, svelmathi@hotmail.com

Graphical Abstract

